

# Real-Time Attitude and Position Estimation for Small UAVs Using Low-Cost Sensors

Derek B. Kingston and Randal W. Beard\*

*Department of Electrical and Computer Engineering  
Brigham Young University, Provo, Utah 84602*

Small unmanned air vehicles (UAVs) and micro air vehicles (MAVs) have payload and power constraints that prohibit heavy sensors and powerful processors. This paper presents real-time attitude and position estimation solutions that use small, inexpensive sensors and low-power microprocessors. In connection with an Extended Kalman Filter attitude estimation scheme, a novel method for dealing with latency in real-time is presented using a distributed-in-time architecture.

Essential to small UAV or MAV missions is the ability to navigate precisely. To reduce computational overhead and to simplify design, a cascaded filter approach to position estimation is used. The design is insensitive to noise and to loss of GPS lock.

Simulation and hardware tests show that the algorithms operate in real-time and are suitable for control, stabilization, and navigation.

## I. Introduction

RECENT interest in design and flight of small UAVs and MAVs has prompted research into control and navigation of such vehicles. The potential for small inexpensive air vehicles is vast: reconnaissance, surveillance, search and rescue, remote sensing (nuclear, biological, chemical), traffic monitoring, natural disaster damage assessment, etc.<sup>1,2</sup> A necessary part of these missions is accurate navigation of the vehicle. Typically, MAVs and small UAVs are very difficult to fly without a trained pilot.<sup>2</sup> To automate the stabilization and navigation of these vehicles, suitable estimation and control schemes are needed. This paper will develop attitude and position estimation filters that use instruments that are small enough to fit on a small UAV (on the order of 50 cm wingspan).

Small UAVs and MAVs have constraints that prohibit traditional solutions to the attitude and position estimation problems. Most notably, accurate navigation-grade gyros are simply too large to be flown on these small aircraft. Power constraints require that low-power embedded microprocessors be used, which can restrict the complexity of algorithms that can be implemented in real-time. One of the contributions of this paper is to show that adequate estimation can be achieved even with these constraints. This solution can also be used as a back-up to more accurate estimation on larger aircraft.

This paper will present a two-stage solution to attitude and position estimation. The first stage is attitude estimation. Many attitude estimation schemes are available. This paper will present a straightforward solution that operates in real-time and satisfies the weight and power constraints of a small UAV. In addition, the attitude estimation scheme will explicitly deal with latency using a unique distributed-in-time formulation. Attitude will be directly available for state feedback, and more importantly, as an input to the second-stage navigation filter. It is notable that with a cascaded filter approach (i.e. the output of the first stage filter feeds the second stage), *any* unbiased attitude estimation scheme can be used at the first stage, including vision-based<sup>2</sup> or infrared-based<sup>3</sup> schemes.

A formulation for an Attitude Heading Reference System (AHRS) will be presented in Section II with simulation results shown in Section III. Section IV contains the Inertial Navigation System (INS) formulation. Section V presents simulation results of the cascaded INS. Results of a hardware experiment are shown in Section VI and Section VII offers conclusions.

---

\*Corresponding author: beard@ee.byu.edu

## II. Real-Time Distributed-in-time AHRS

THE purpose of this section is to present a real-time solution to the attitude estimation problem in the presence of delayed measurements.<sup>a</sup> We implement an Extended Kalman Filter (EKF), but complementary filters and Unscented Kalman Filters (UKF)<sup>5</sup> could also be used. To formulate an EKF, a state-space model of the system along with a mathematical description of the relationship between measurements and state variables must be available.

### A. Attitude Filtering

The attitude dynamics of a rigid body can be described in terms of the unit quaternion vector,<sup>6</sup>  $\mathbf{q}$ , by

$$\dot{\mathbf{q}} = \mathbf{\Omega}(\boldsymbol{\omega})\mathbf{q} \quad (1)$$

where  $\mathbf{q}$  is the attitude quaternion vector and

$$\mathbf{\Omega}(\boldsymbol{\omega}) = \frac{1}{2} \begin{bmatrix} 0 & -\omega_1 & -\omega_2 & -\omega_3 \\ \omega_1 & 0 & \omega_3 & -\omega_2 \\ \omega_2 & -\omega_3 & 0 & \omega_1 \\ \omega_3 & \omega_2 & -\omega_1 & 0 \end{bmatrix} \quad (2)$$

where  $\omega_1$  is the roll rate,  $\omega_2$  the pitch rate, and  $\omega_3$  the yaw rate.

To avoid the need to know the inertia tensor of the vehicle (needed to compute angular accelerations) we use rate gyro measurements to update the quaternion estimate. While this introduces noise and other complications, it allows an implementation that is general for a large range of vehicles. Small UAVs and MAVs have very small payload capacity which necessitates the use of small MEMS devices to measure angular rates. These devices drift over time. Because the estimate of  $\mathbf{q}$  is effectively the integral of the rate gyros (1), some compensation for drift will be needed to give a reliable estimate. Without an estimate of bias, the discrepancy between measured attitude and the attitude obtained through Equation (1) will grow, causing the filter to diverge. For this reason the state vector is given by

$$\mathbf{x} = \begin{bmatrix} \mathbf{q} \\ \mathbf{b} \end{bmatrix} \quad (3)$$

where  $\mathbf{q}$  is the quaternion estimate of attitude and  $\mathbf{b}$  is the estimate of bias on the rate gyros. By explicitly estimating the bias on the rate gyros, compensated angular rates can be made available to the UAV controller. The drift on gyros can be modelled as a random walk, so the state-space model is simply  $\dot{\mathbf{b}} = \mathbf{0}$ . The system is then described by

$$\begin{aligned} \dot{\mathbf{x}} &= \mathbf{f}(\mathbf{x}, \boldsymbol{\omega}) \\ \mathbf{y} &= \mathbf{h}(\mathbf{x}) \end{aligned} \quad (4)$$

where

$$\mathbf{f}(\mathbf{x}, \boldsymbol{\omega}) = \begin{bmatrix} \mathbf{\Omega}(\boldsymbol{\omega} - \mathbf{b})\mathbf{q} \\ \mathbf{0}_{3 \times 1} \end{bmatrix}, \quad \mathbf{h}(\mathbf{x}) = \begin{bmatrix} \tan^{-1} \left( \frac{2(q_2q_3 + q_0q_1)}{1 - 2(q_1^2 + q_2^2)} \right) \\ \sin^{-1}(-2(q_1q_3 - q_0q_2)) \\ \tan^{-1} \left( \frac{2(q_1q_2 + q_0q_3)}{1 - 2(q_2^2 + q_3^2)} \right) \end{bmatrix} = \begin{bmatrix} \phi \\ \theta \\ \psi \end{bmatrix} \quad (5)$$

and  $\boldsymbol{\omega}$  is the vector of angular rates measured by the gyros and  $\mathbf{h}(\mathbf{x})$  is the transformation from quaternion to Euler representation of attitude.<sup>7</sup> This transformation is needed because the measured values of attitude will be represented with Euler angles and because quaternion errors can be difficult to make sense of.<sup>8,5</sup>

---

<sup>a</sup>For a detailed explanation see<sup>4</sup>

## B. Attitude Measurements

One of the most difficult parts to estimating attitude is obtaining a measurement. A number of different solutions to the attitude measurement problem have been proposed and implemented. One popular method is to use the carrier phase of GPS signals.<sup>9,10</sup> This involves at least three GPS antennas with a known geometry. Once the phase ambiguity is resolved, phase differences between antennas can be calculated and a good estimate of attitude is made. The solution improves as the baseline between antennas increases, making implementation on small UAVs or MAVs difficult. Gebre-Egziabher et al<sup>11</sup> proposed an ultra short baseline solution (approx 36 cm baseline), but even this is too large and heavy for small UAVs and MAVs.<sup>2,12</sup> Other promising methods for small UAVs and MAVs use vector measurements of the magnetic and gravitational fields and then solve a set of nonlinear equations using optimization methods to come up with an attitude measurement.<sup>8,13</sup> A unique approach is to use the signal-to-noise ratio on the GPS antenna to measure attitude.<sup>14</sup> Because the end goal of estimating attitude is usually to control or stabilize the aircraft (i.e. use the estimate as state feedback), Akella et al<sup>15</sup> formulated a feedback law that skips the estimation step and regulates the attitude with only gyro and inclinometer measurements.

Perhaps the most straight-forward way to measure attitude is to use the accelerometers as an inclinometer to give a measurement of roll ( $\phi$ ) and pitch ( $\theta$ ) with the direction of GPS velocity used to measure heading ( $\psi$ ). Complications arise, however, due to the aircraft acceleration in the reference frame. This means that the accelerometers will not measure the gravity vector, rather they will measure the aircraft apparent gravity ( $\mathbf{g} - \mathbf{a}_{\text{aircraft}}$ ). By augmenting accelerometer measurements with GPS calculated accelerations a good estimate of roll and pitch can be made.<sup>8,16</sup> In addition, the use of GPS to calculate heading will only work if the aircraft has a velocity from which to calculate heading, therefore, the AHRS presented in this paper will only be valid for fixed-wing aircraft flying at velocities high enough to generate a GPS heading angle. This limitation can be overcome with the addition of a magnetic compass, but for aircraft where GPS heading is reliable, the extra hardware and complexity may not be desirable.

Measurements of  $\phi$  and  $\theta$  are made by measuring the acceleration in the body frame and relating it to a reference acceleration vector in the Earth Centered Earth Fixed (ECEF) frame (usually the gravity vector  $\mathbf{g} = [0 \ 0 \ g]^T$ , where  $g$  is the gravitational constant). The reference vector is constructed such that when the reference vector is measured in the body frame, this will correspond to zero roll and zero pitch angles.

To relate the measured acceleration in the body frame to the reference vector in the ECEF frame, a mathematical relationship between the two should be formalized. The rotation matrix from the ECEF frame to the body frame is

$$\mathcal{C}_{\text{ECEF} \rightarrow \text{body}} = \begin{bmatrix} \cos(\theta) & 0 & -\sin(\theta) \\ \sin(\theta) \sin(\phi) & \cos(\phi) & \cos(\theta) \sin(\phi) \\ \sin(\theta) \cos(\phi) & -\sin(\phi) & \cos(\theta) \cos(\phi) \end{bmatrix} \quad (6)$$

and it follows that the transformation of acceleration in the ECEF frame to acceleration in the body frame is

$$\begin{bmatrix} a_x \\ a_y \\ a_z \end{bmatrix} = \mathcal{C}_{\text{ECEF} \rightarrow \text{body}} \begin{bmatrix} r_x \\ r_y \\ r_z \end{bmatrix} \quad (7)$$

where  $\mathbf{a}$  is in the body frame and  $\mathbf{r}$  is in the ECEF frame.

When the aircraft (and hence the body frame) is accelerating relative to the ECEF frame, the accelerometers will not measure the gravity vector, rather they will measure the aircraft apparent gravity ( $\mathbf{g} - \mathbf{a}_{\text{aircraft}}$ ). The acceleration of the aircraft relative to the ECEF frame,  $\mathbf{a}_{\text{aircraft}}$ , is the second derivative of GPS measurements rotated by the heading  $\psi$ . The rotation by  $\psi$  is necessary to align the  $X$  and  $Y$  GPS measurements with the body  $X$  and  $Y$  axes. With knowledge of this acceleration, a new reference vector can be constructed

and  $\phi$  and  $\theta$  can be solved for as follows:

$$\begin{aligned}
r_x &= -(\cos(\psi)a_{\text{GPS}_x} + \sin(\psi)a_{\text{GPS}_y}) \\
r_y &= -(-\sin(\psi)a_{\text{GPS}_x} + \cos(\psi)a_{\text{GPS}_y}) \\
r_z &= g - a_{\text{GPS}_z} \\
\sigma_\theta &= \frac{r_x a_x + r_z \sqrt{r_x^2 + r_z^2 - a_x^2}}{r_x^2 + r_z^2} \\
\theta &= \tan^{-1} \left( \frac{\sigma_\theta r_x - a_x}{\sigma_\theta r_z} \right) \tag{8}
\end{aligned}$$

$$\begin{aligned}
r_\theta &= r_x \sin(\theta) + r_z \cos(\theta) \\
\sigma_\phi &= \frac{r_y a_y + r_\theta \sqrt{r_y^2 + r_\theta^2 - a_y^2}}{r_y^2 + r_\theta^2} \\
\phi &= \tan^{-1} \left( \frac{-\sigma_\phi r_y + a_y}{\sigma_\phi r_\theta} \right). \tag{9}
\end{aligned}$$

The procedure for obtaining an attitude measurement using a low-cost GPS receiver and three axis accelerometers is now addressed. While many GPS receivers can be configured to output velocities as well as positions, it will be assumed that the GPS receiver outputs only position information at 1 Hz.

To make a measurement of attitude the following steps are followed:

1. Obtain three consecutive GPS position measurements,
2. Difference the GPS measurements to obtain two velocity measurements,
3. Average the velocity measurements to give average velocity over 2 seconds,
4. Calculate the heading  $\psi$  from velocity:

$$\psi = \tan^{-1} \left( \frac{\dot{Y}}{\dot{X}} \right), \tag{10}$$

5. Difference the GPS calculated velocities to obtain a GPS acceleration measurement  $\rightarrow \mathbf{a}_{\text{GPS}}$ ,
6. Average the accelerometers over the same 2 seconds as the GPS velocity is calculated  $\rightarrow \mathbf{a}$ ,
7. Calculate roll  $\phi$  and pitch  $\theta$  using the accelerometers and GPS acceleration rotated by  $\psi$  using Equations (8) and (9).

### C. Latency and Real-Time Computation

When measurements are made in the manner outlined in section II.B, significant latency is introduced. To evaluate the latency of a measurement, it is assumed that a GPS receiver outputs positions at a rate of 1 Hz with latency of approximately 1/10th of a second (due to calculation onboard the GPS module and communication from the GPS receiver to the microprocessor).

Referring to Figure 1, by the time the information is available to make a measurement of attitude, the measurement will be delayed by 1.1 seconds. Note that to make the measurement, accelerometer values need to be known from the time the first GPS position considered was received – this requires logging of accelerometer measurements over a 2.1 second interval.

To compensate for latency, it is proposed that all sensor and state information be data logged over the 2.1 second period from which GPS acceleration will be calculated. Once a measurement is generated (with latency of 1.1 seconds), the state estimate corresponding to 1.1 seconds previous is updated. The updated estimate is then propagated using the stored sensor information up to the current time.

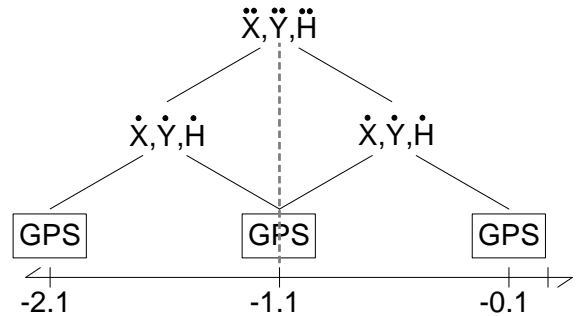


**Figure 1. Latency from GPS acceleration calculation.**

The propagation of the state from the measurement update up to the current time will dominate the computation time required to run the filter. For most systems, there will not be enough computational ability to do this without significantly reducing the sample rate. To address latency while simultaneously allowing for a fast filter update rate, a distributed-in-time computation architecture is used. Figure 2 outlines the design of a distributed-in-time filter.

The idea is to only call the time update routine often enough each time step to ensure real-time capability while also guaranteeing that the updated estimate reaches current-time before the next measurement is made. Essentially, we use the empty time during the iterations between measurement updates to propagate the latent estimate up in time. While the updated estimate is being propagated in time, a previous best estimate should also be propagated to make the best no-latency estimate available until the updated estimate has zero latency.

To illustrate the distributed-in-time architecture and to demonstrate real-time capability, an implementation of the AHRS has been designed and tested. The target filter update rate is 30 Hz. A low-power microcontroller running at 29 MHz was used. On this platform, the time update takes 3.75 milli-seconds and the measurement update takes 9 milli-seconds. With these computational constraints and without a distributed-in-time architecture, the filter could not address latency without bringing the filter update rate down to below 15 Hz. To design a 30 Hz update rate, the computation dealing with latency is spread over multiple updates of the filter, with the computation for each step not to exceed 33 milli-seconds.

Figure 3 shows how the computation is distributed to ensure a no-latency estimate at 30 Hz. Note that the measurement updated estimate gets propagated 33 times (corresponding to the 1.1 seconds of latency) over 5 updates of the filter. A no-latency EKF with these computational constraints could be designed to run at 78 Hz – the same rate that a normal EKF could run. In fact, a no-latency filter can run at the same rate as its counterpart if the time required for a measurement update is greater than or equal to twice the time required for a time update and the latency in the measurement is less than twice the time between measurements.

Note that, in general, the time required to do a measurement update will be larger than the time required to perform a time update (due to the need to invert a matrix during the measurement update). Often, latent measurements have small latency compared to the time between measurements, so a no-latency EKF will, in many cases, be able to operate at the same rate as its counterpart.

### III. AHRS Simulation Results

THIS section describes simulation results of the AHRS formulated in section II. A full 6 degree of freedom model provides truth values. The simulated aircraft performed an 11 minute flight with multiple coordinated turn and climb maneuvers. Figure 4 shows the roll angle over the simulated flight (pitch and yaw angles show similar noise characteristics). The solid line is the true roll angle and the dashed line is the estimate from the AHRS.

Noise values on simulated sensors are selected based on manufacturer specifications and experimental data. Noise values are modelled as Gaussian  $\mathcal{N}(0, \sigma^2)$ , drift values are modelled as Random Walk (i.e.  $\int \mathcal{N}(0, \sigma^2)$ ), and GPS is modelled as a Gauss-Markov Process with delay of 1/10th of a second and a correlation time of 100 seconds. The simulated standard deviation for the gyro drift is  $3^\circ/\text{sec}/\text{min}$ .

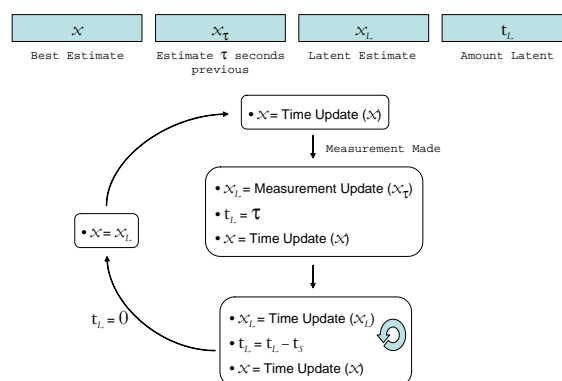


Figure 2. Distributed-in-time filter architecture.

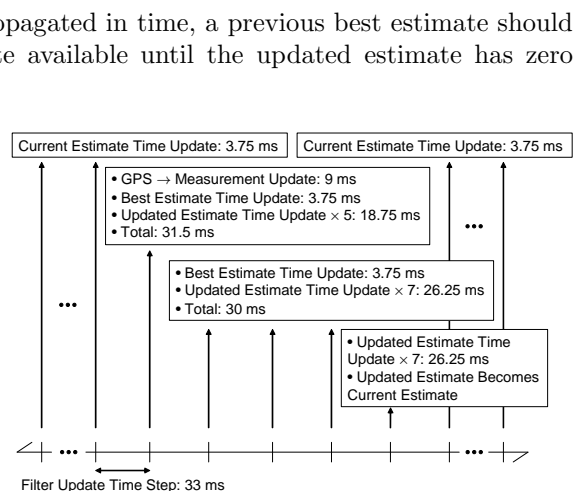


Figure 3. Latency compensation at 30 Hz.

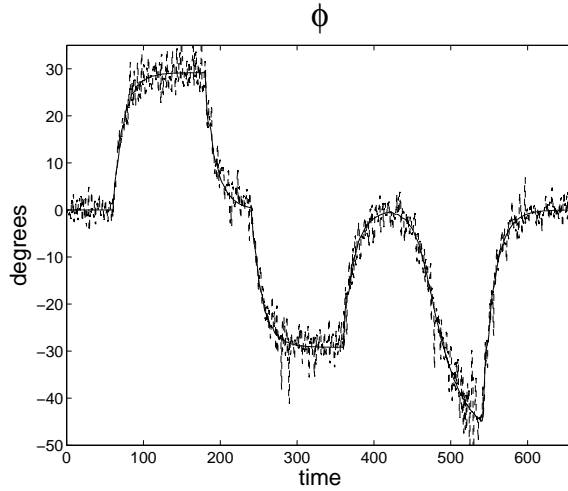


Figure 4. Roll angle over 11 minute flight.

The AHRS is able to estimate the roll, pitch, and yaw angles with zero mean and standard deviation of approximately  $3^\circ$ . Similarly, the bias estimates have standard deviation of  $0.84^\circ/\text{sec}$ .

#### IV. Cascaded INS Filter

THE choice of cascading an AHRS filter with a separate INS filter is based primarily on the ease of design and computational efficiency. In a cascaded format, the AHRS and INS filters can be designed and tuned completely independent of each other. The relationship between the two filters can be described succinctly (and fairly accurately) by the input noise parameters to the INS filter. A cascaded structure also reduces computation. By removing the calculations that relate the attitude states to the inertial states, the cascade formulation has much less computational overhead than a full EKF. Even though the cascaded filter is sub-optimal,<sup>17,18</sup> the performance is comparable to the full EKF. In other words, the cascade implementation allows for increased flexibility, is easier to implement and tune, and is dramatically less computationally expensive, with only a small performance loss.

The general UAV equations of motion<sup>19</sup> for navigation are

$$\begin{bmatrix} \dot{X} \\ \dot{Y} \\ \dot{Z} \end{bmatrix} = \text{DCM}^T \begin{bmatrix} u \\ v \\ w \end{bmatrix} \quad (11)$$

$$\begin{bmatrix} \dot{u} \\ \dot{v} \\ \dot{w} \end{bmatrix} = \text{DCM} \begin{bmatrix} 0 \\ 0 \\ g \end{bmatrix} + \frac{1}{m} \mathbf{F} - \begin{bmatrix} p \\ q \\ r \end{bmatrix} \times \begin{bmatrix} u \\ v \\ w \end{bmatrix} \quad (12)$$

where DCM is the Direction Cosine Matrix;<sup>6</sup>  $u$ ,  $v$ , and  $w$  are the body velocities out the nose, the right wing, and the belly, respectively;  $X$  and  $Y$  are the inertial coordinates of the UAV in the Earth Centered Earth Fixed (ECEF) frame;  $-Z$  is altitude;  $g$  is the gravitational constant;  $m$  is the mass of the UAV;  $\mathbf{F}$  is the translational forces acting on the UAV;  $p$ ,  $q$ , and  $r$  are the roll, pitch, and yaw rates, respectively.

A typical AHRS/INS filter will propagate the states in Equations (11) and (12) along with attitude and gyro bias states. This can be problematic because the  $\mathbf{F}/m$  term can be hard to characterize. Many implementations simply use accelerometers to estimate this term, but this is basically integrating the accelerometers twice to get position – any small drift in the accelerometers can cause problems. To avoid this and to break the filter into a cascaded format, the following assumptions will be made: (1) attitude is available from a preceding AHRS filter, (2)  $v$  and  $w$  are much less than  $u$  and close to zero (this is equivalent to assuming small angle of attack and very little sideslip), and (3) a measurement of altitude is available

even when GPS lock has been lost (say from an absolute pressure sensor). With these assumptions in place, the cascaded INS filter takes the form given in Figure 5 where  $V_p$  is measure airspeed.

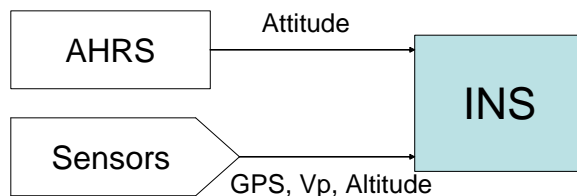


Figure 5. Diagram of Cascaded INS

Treating the attitude estimate from the AHRS and the UAV airspeed as an inputs to the INS, the state-space model of position is given by

$$\dot{\mathbf{x}} = \text{DCM}^T \begin{bmatrix} V_p \\ 0 \\ 0 \end{bmatrix}, \quad \mathbf{y} = \mathbf{x} \quad (13)$$

where the DCM is the rotation matrix that maps vectors from the reference frame to the body frame (purely a function of attitude) and  $\mathbf{x} = [X \ Y \ Z]^T$ .

In forming the INS, note that the inertial states are driven by the body velocities rotated by the attitude (Equation (11)). Treating attitude as the input to this filter allows us to form the DCM from the inputs, reducing the computation associated with calculating the statistical relationship between attitude changes and the resulting change in position. Using this same notion of reduction of complexity by replacing states, we can replace the vector  $[u \ v \ w]^T$  by  $[V_p \ 0 \ 0]^T$  where  $V_p$  is the measured airspeed. In this way, we avoid the complex state update in Equation (12) as well as the problematic measurement of  $[u \ v \ w]^T$  (which would require angle of attack and angle of sideslip sensors).

Note that  $u$ ,  $v$ , and  $w$  are all inputs, with  $u \approx V_p$  and  $v, w \approx 0$ . By defining noise characteristics for all attitude inputs as well as for  $u$ ,  $v$  and  $w$  estimates, the relationship from input to state changes can be leveraged by the EKF.

The advantages of an INS in this format are very low computational overhead and insensitivity to loss of GPS or noisy inputs from attitude and airspeed.

## V. INS Simulation Results

THE INS presented in Section IV was simulated in the same manner as the AHRS to determine accuracy of the INS filter. The INS was also programmed in C code for a 29 MHz low-power microprocessor. Real-time ability of the INS is demonstrated by the execution times of the INS on this platform: 2 milli-seconds for both time and measurement updates.

Two flight tests were simulated; one where GPS was available for the full time and one where GPS information was ignored for the remainder of the flight after the filter had run for a short time. Figure 6(a) shows the filter results with the corresponding GPS measurements for the case when GPS connection is uninterrupted. A magnified portion of the data is shown to verify that the INS correctly smoothes through GPS measurements, providing an estimate of position at every instant of time. Figure 6(b) shows the case when GPS lock is lost halfway through the flight. As can be seen, even after 5 minutes of no GPS lock, the INS only strays a maximum of 22 meters from the true position. In both figures the solid line is the true position and the dashed line is the estimated position from the INS.

The performance of the INS is very good considering the quality of the inputs (standard deviation of attitude angles of  $5^\circ$  and on airspeed 4 m/s). It is concluded that the INS is robust to both input noise and GPS loss.

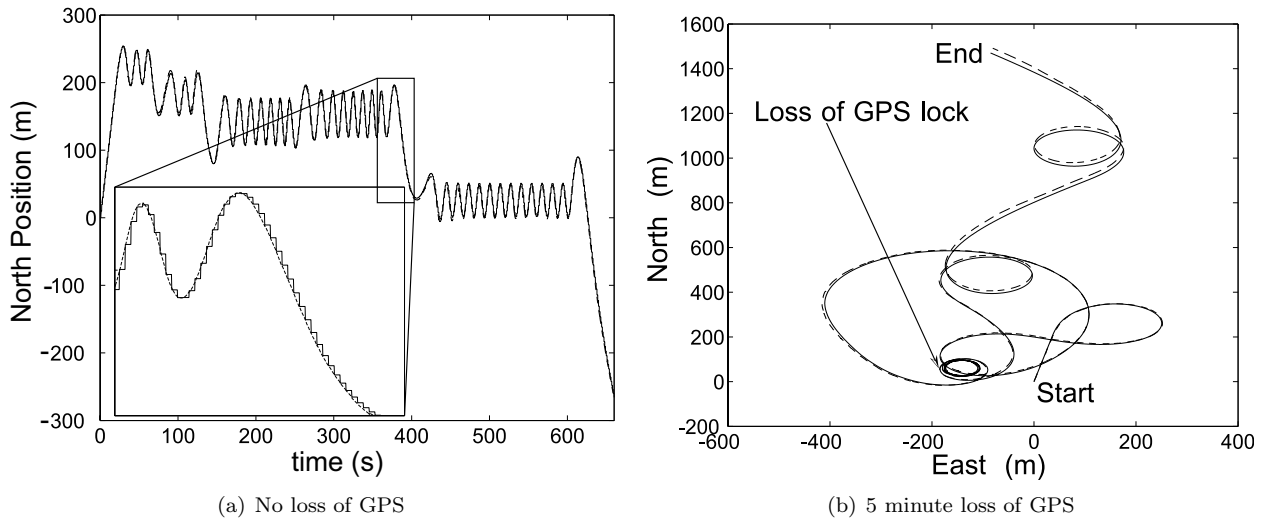


Figure 6. INS performance in simulation

## VI. Preliminary Hardware Results

To verify the results obtained through simulation, a hardware experiment was performed. A suite of sensors identical to those used in BYU's low-cost autopilot<sup>20</sup> is placed in a cradle at the end of a 2.5 meter boom. A motor drives the setup at variable speeds in a circle – effectively putting the sensors in a coordinated turn. Truth values for roll angle are obtained through a potentiometer attached to the cradle; pitch angle is assumed to be zero due to the mounting of the sensors in the cradle. Truth values for inertial position and heading angle are obtained through integrating the encoder on the driving motor and using the geometry of the setup. As can be seen in Figure 7(a), the AHRS estimates roll and pitch angles to within 2 degrees. Figure 7(b) shows that the performance of the INS is also very accurate. It should be emphasized that these results were obtained with actual hardware sensors and in a manner that very closely approximates actual coordinated flight.

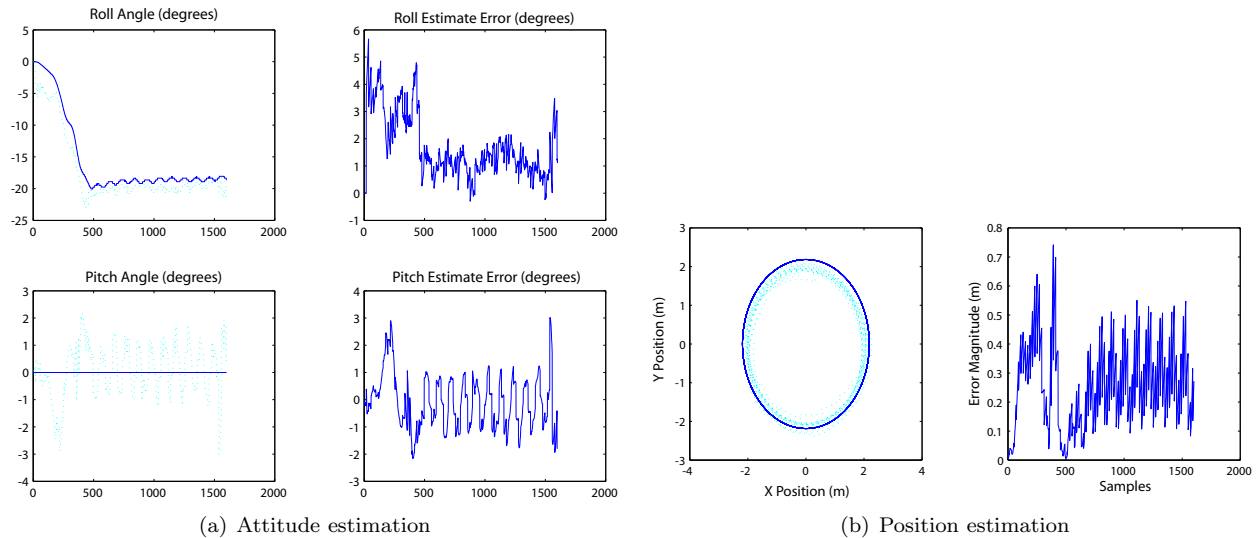


Figure 7. AHRS and INS results during a preliminary hardware experiment

## VII. Conclusions

FOR small UAV and MAV applications, payload is critical. The AHRS and INS as outlined in this paper require only very light-weight, inexpensive sensors. The total sensor payload including the GPS receiver is less than 0.45 oz. (12.7 grams).<sup>20</sup> With future miniaturization, a complete sensor suite plus microprocessor could possibly be developed to be small enough to be flown on a MAV. A current hardware implementation at BYU weighs 2.2 oz. and has demonstrated autonomous flight on aircraft with wingspans as small as 21 in.

This paper has demonstrated a real-time solution to attitude and position estimation for small UAVs and MAVs. A real-time AHRS has been developed that explicitly deals with latency and has been shown to be adequate for small UAV and MAV applications. A cascaded filter implementation of an INS has been demonstrated in simulation and preliminary hardware tests and has been shown to be insensitive to GPS loss and input noise.

## References

- <sup>1</sup>Fontana, R. J., Richley, E. A., Marzullo, A. J., Beard, L. C., Mulloy, R. W. T., and Knight, E. J., "An ultra wideband radar for micro air vehicle applications," *Proceedings of the IEEE Conference on Ultra Wideband Systems and Technologies*, 2002, pp. 187–191.
- <sup>2</sup>Ettlinger, S. M., Nechyba, M. C., Ifju, P. G., and Waszak, M., "Vision-guided flight stability and control for micro air vehicles," *Proceedings of the IEEE/RSJ International Conference on Intelligent Robots and System*, Vol. 3, 2002, pp. 2134–2140.
- <sup>3</sup>Taylor, B., Bil, C., Watkins, S., and Egan, G., "Horizon Sensing Attitude Stabilisation: A VMC Autopilot," *International UAV Systems Conference*, Bristol, UK, 2003.
- <sup>4</sup>Kingston, D. B., *Implementation Issues of Real-Time Trajectory Generation on Small UAVs*, Master's thesis, Brigham Young University, Provo, Utah 84602, April 2004, <http://www.ee.byu.edu/magicc/publications/thesis/DerekKingston.pdf>.
- <sup>5</sup>Crassidis, J. L. and Markley, F. L., "Unscented Filtering for Spacecraft Attitude Estimation," *Journal of Guidance, Control, and Dynamics*, Vol. 26, August 2003, pp. 536–542.
- <sup>6</sup>Wertz, J. R., editor, *Spacecraft Attitude Determination and Control*, D. Reidel Publishing Company, Dordrecht, Holland, 1978.
- <sup>7</sup>MathWorks, "Euler Angles to Quaternions," <http://www.mathworks.com/access/helpdesk/help/toolbox/aeroblks/euleranglestoquaternions.shtml>.
- <sup>8</sup>Gebre-Egziabher, D., Elkaim, G. H., Powell, J. D., and Parkinson, B. W., "A Gyro-Free Quaternion-Based Attitude Determination System Suitable for Implementation Using Low Cost Sensors," *Proceedings of the IEEE Position, Location, and Navigation Symposium*, San Diego, CA, March 2000, pp. 185–192.
- <sup>9</sup>Peng, H. M., Chiang, Y. T., Chang, F. R., and Wang, L. S., "Maximum-Likelihood-Base Filtering for Attitude Determination via GPS Carrier Phase," *Proceedings of the IEEE Position, Location, and Navigation Symposium*, San Diego, CA, March 2000, pp. 480–487.
- <sup>10</sup>Chiang, Y. T., Wang, L. S., Chang, F. R., and Peng, H. M., "Constrained filtering method for attitude determination using GPS and gyro," *Proceedings of the IEEE Radar, Sonar and Navigation*, Vol. 149, October 2002, pp. 285–264.
- <sup>11</sup>Gebre-Egziabher, D., Hayward, R. C., and Powell, J. D., "A low-cost GPS/inertial attitude heading reference system (AHRS) for general aviation applications," *Proceedings of the IEEE Position Location and Navigation Symposium*, Palm Springs, CA, April 1998, pp. 518–525.
- <sup>12</sup>Motazed, B., Vos, D., and Drela, M., "Aerodynamics and flight control design for hovering micro air vehicles," *Proceedings of the IEEE American Control Conference*, Vol. 2, Philadelphia, PA, June 1998, pp. 681–683.
- <sup>13</sup>Marins, J. L., Yun, X., Bachmann, E. R., McGhee, R. B., and Zyda, M. J., "An extended Kalman filter for quaternion-based orientation estimation using MARG sensors," *Proceedings of the IEEE/RSJ International Conference on Intelligent Robots and Systems*, Vol. 4, Maui, HI, October 2001, pp. 2003–2011.
- <sup>14</sup>Lightsey, E. G. and Madsen, J., "Three Axis Attitude Determination Using GPS Signal to Noise Ratio Measurements," *AIAA Journal of Guidance, Control and Dynamics*, Vol. 26, April 2003, pp. 304–310.
- <sup>15</sup>Akella, M. R., Halbert, J. T., and Kotamraju, G. R., "Rigid body attitude control with inclinometer and low-cost gyro measurements," *Elsevier Systems and Control Letters 49*, Santa Barbara, CA, February 2003, pp. 151–159.
- <sup>16</sup>Vaganay, J., Aldon, M. J., and Fournier, A., "Mobile robot attitude estimation by fusion of inertial data," *Proceedings of the IEEE International Conference on Robotics and Automation*, Vol. 1, Atlanta, GA, May 1993, pp. 277–282.
- <sup>17</sup>Carlson, N. A., "Federated Square Root Filter for Decentralized Parallel Processes," *Proceedings of the IEEE National Aerospace and Electronics Conference*, Dayton, Ohio, May 1987, pp. 1448–1456.
- <sup>18</sup>Schlee, F. H., Toda, N. F., Islam, M. A., and Standish, C. J., "Use of an external cascade Kalman filter to improve the performance of a Global Positioning System (GPS) inertial navigator," *Proceedings of the IEEE Aerospace and Electronics Conference*, Dayton, OH, May 1988, pp. 345–350.
- <sup>19</sup>Roskam, J., *Airplane Flight Dynamics and Automatic Flight Controls*, Design, Analysis and Research Corporation, Lawrence, KS, 2001.
- <sup>20</sup>Kingston, D. B., Beard, R. W., McLain, T. W., Larsen, M., and Ren, W., "Autonomous Vehicle Technologies for Small Fixed Wing UAVs," *AIAA 2nd Unmanned Unlimited Systems, Technologies, and Operations—Aerospace, Land, and Sea Conference and Workshop & Exhibit*, San Diego, CA, September 2003, AIAA Paper No. 2003-6559.